Intracellular Ruthenium-Promoted (2+2+2) Cycloadditions

Joan Miguel-Ávila, María Tomás-Gamasa,* and José L. Mascareñas*

In memory of Professor Kilian Muñiz

Abstract: *Metal-mediated intracellular reactions are becoming invaluable tools in chemical and cell biology, and hold promise for strongly impacting the field of biomedicine. Most of the reactions reported so far involve either uncaging or redox processes. Demonstrated here for the first time is the viability of performing multicomponent alkyne cycloaromatizations inside live mammalian cells using ruthenium catalysts. Both fully intramolecular and intermolecular cycloadditions of diynes with alkynes are feasible, the latter providing an intracellular synthesis of appealing anthraquinones. The power of the approach is further demonstrated by generating anthraquinone AIEgens (AIE = aggregation induced emission) that otherwise do not go inside cells, and by modifying the intracellular distribution of the products by simply varying the type of ruthenium complex.*

Introduction

Cells can be viewed as complex, tiny factories performing thousands of simultaneous chemical reactions.[1] As chemists, we are not bound to reproduce natural processes, and can therefore aspire at conducting non-coded catalytic reactions within living environments. While native enzymatic transformations are unbeatable with regard to rate and selectivity, abiotic catalytic processes might be advantageous in terms of versatility and substrate scope.[2] Furthermore, introducing non-natural reactivity in cellular contexts can provide unprecedented opportunities for cellular and metabolic intervention.[3] However, performing exogenous catalytic reactions within living cells is far from trivial, as it requires to maneuver among multitude of components and functional groups, and in an aqueous, crowded and compartmentalized environment.

For many years, it was considered that organometallic catalysis was incompatible with aqueous and biological environments; however, the last decade has witnessed an increasing number of reports on bioorthogonal, and even intracellular transformations, mediated by transition metals.[4] However, the repertoire of reactions is yet scarce, and mainly limited to uncaging processes;[5] albeit other reactions, like reductions,[6] isomerizations[7] and cyclizations,[8] have also been recently introduced. Therefore, there is a great interest in increasing the repertoire of metal-mediated reactions that can be performed in live settings, as this will contribute to further establish this field, and expand its biotech and biomedical potential. A particularly attractive type of transformations are cycloaddition reactions, owing to their synthetic power, and the lack natural counterparts, albeit there have been claims on the existence of Diels–Alderases.[9]

Intracellular cycloadditions promoted by transition metals have been limited to sporadic applications of the renowned copper-mediated alkyne-azide cycloaddition (*CuAAC*) (Figure 1, i),[10] a key reaction for the establishment of the field of bioorthogonal chemistry.[11] Unfortunately, its efficiency in intracellular settings is compromised by the toxicity and oxidation lability of copper. We recently developed a ruthe-

[*] J. Miguel-Ávila, Dr. M. Tomás-Gamasa, Prof. J. L. Mascareñas
Centro Singular de Investigación en Química Biolóxica e Materiais Moleculares (CIQUS), and Departamento de Química Orgánica, Universidade de Santiago de Compostela
15782 Santiago de Compostela (Spain)
E-mail: maria.tomas@usc.es
joseluis.mascarenas@usc.es

Supporting information and the ORCID identification number(s) for the author(s) of this article can be found under:
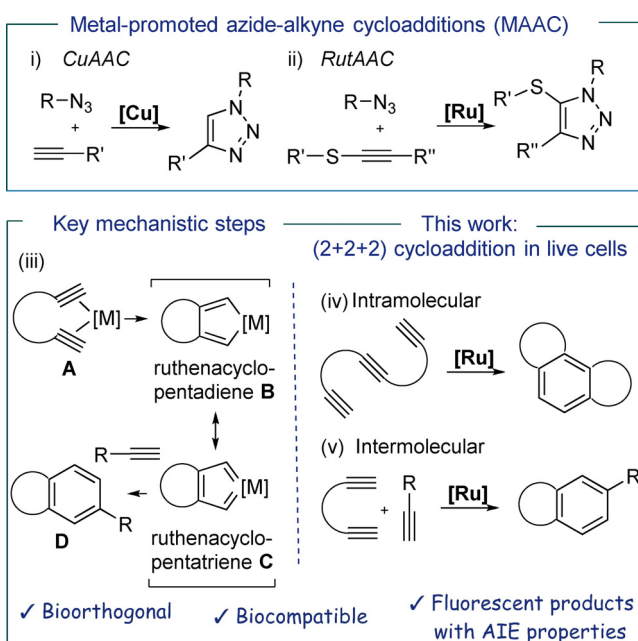https://doi.org/10.1002/anie.202006689.

Figure 1. Top: i) *CuAAC*, feasible in living mammalian cells using specific formulations of Cu;[10] ii) *RutAAC*, can be performed in cell lysates.[12] Bottom: Left: mechanistic rational behind the orthogonality of the proposed cycloaddition; Right: (2+2+2) cycloadditions.

nium-mediated alternative that involves thioalkynes as azide partners (Figure 1, ii). However, it couldn't be implemented inside living cells.[12]

At some point of our research we envisioned that moving from alkynes to appropriately tethered diynes, there might be better chances for bioorthogonal "fishing" of transition metal reagents owing to the bidentate coordination ability of the substrate (**A**, Figure 1).[13] An ensuing oxidative cyclometal-lation would give a metallacycle (**B/C**, Figure 1) that could be trapped by another alkyne to provide aromatic adducts formally resulting from a (2+2+2) cycloaddition (**D**, Figure 1, iii). This type of cyclotrimerization of alkynes is well-known in the realm of synthetic chemistry,[14] and has also been even accomplished in aqueous media, using Co, Rh, or Ru catalysts;[15,16] but never in a cellular context.

In this manuscript we demonstrate the viability of this process, by reporting the first examples of a multicomponent cycloaddition carried out in the interior of live, unfixed mammalian cells. The reaction, which is mediated by non-toxic ruthenium complexes, allows to make three C–C bonds, and at least two new cycles, in a single step, therefore enabling a remarkable increase in structural complexity.

We demonstrate that the cyclotrimerization is not only viable in fully intramolecular cases, but also when using isolated alkynes as external reaction partners (Figure 1, iv and v). Remarkably, this latter reaction allows to generate "in cellulae" anthraquinones, secondary metabolites which cannot be produced by mammalian cells. We also demonstrate that whereas anthraquinone derivatives with AIE (aggregation induced emission) characteristics do not internalize, they can be indirectly "introduced" inside cells using our reaction. We can even go one step further and promote the preferential generation of cycloadducts in different intracellular locations.

Results and Discussion

Our initial experiments were planned considering previous work of Cadierno and co-workers,[15b] and of Teply,[16] demonstrating the viability of achieving cyclotrimerizations of alkynes under different aqueous conditions, using [RuCp*Cl(COD)] (**Ru1**) as catalyst. However, these reactions were carried out using relatively high concentration of reactants, and required long reaction times, which raised doubts on their exportability to biological environments. We first tested the cyclotrimerization of triyne **1**, because it is an intramolecular process, and the resulting pentacyclic product **2** is fluorescent (Figure 2a), thereby providing for tracking the reaction using microscopy. After some optimization, we managed to accomplish the reaction in complex biological media such as phosphate-buffered saline solution (PBS), cell culture media (DMEM) and HeLa cell lysates, even using micromolar concentrations of the precursor (Figure 2a).

We then moved to a real biological scenario, a mammalian living cell. Therefore, HeLa cells were incubated with **Ru1** and washed twice with DMEM to remove the excess of the complex. The presence of ruthenium inside cells was confirmed by ICP-MS analysis (Figure S17). Then, cells were mixed with substrate **1** for 1 h. Panel A in Figure 2b displays

a) Intramolecular (2+2+2) Ru-mediated cycloaddition[a]

	% yield
PBS	52
DMEM	41
Lysates[b]	32
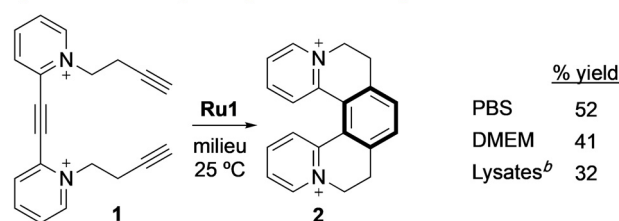
b) Intracellular generation of product **2**
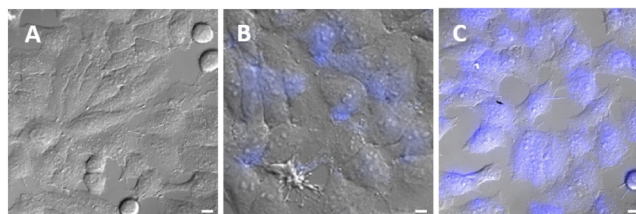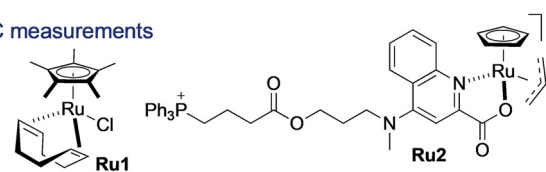

c) CTFC measurements

Figure 2. a) Ruthenium-mediated annulation of triyne **1** in aqueous buffers. b) Fluorescence micrographies of Hela cells (brightfield) after incubation with: A) **1**; B) **Ru1**, washed, and treated with **1**; C) **Ru2**, washed, and treated with **1**; conditions: cells were incubated with [**Ru**] (50 µM) for 30 min, followed by two washings with DMEM, and treatment with substrate **1** (100 µM) for 1 h. Blue channel: $\lambda_{exc} = 385$ nm, $\lambda_{em} = 410$–480 nm. c) CTCF measurements (corrected total cell fluorescence). Error bars from three independent experiments. Scale bar: 12.5 µm. [a] Performed using substrate **1** (5 mmol), milieu (5.0 mL), **Ru1** (25 mol%), 25 °C, 24 h; Yields determined by NMR spectroscopy using an internal standard. [b] Cell lysates 6 mg mL^{-1}. Note: counterions in **Ru2** should be Br$^-$ and PF$_6^-$.

the cells after treatment only with substrate **1**, which show no fluorescence. In contrast, we did observe some fluorescence in cells that had been pretreated with **Ru1** (panel B), in agreement with the formation of the product **2**. Remarkably, using the complex **Ru2**, which we knew from previous studies that presents a good cellular uptake and tolerance,[5e] we observed a more intense intracellular emission (Figure 2b, panel C), consisting with the generation of a larger amount of product. Indeed, we calculated a three-fold higher fluorescence intensity when compared with that resulting from the use of **Ru1** (Figure 2c). The ruthenium (IV) complex **Ru2** is likely reduced in situ to an active Ru^{II} species;[5d] and its better performance in cells seems in part associated to an improved uptake with respect to **Ru1** (Section S12). The processes didn't produce observable changes in the morphology of the cells or affect the survival at the operating times (Figure S8).

The above results are consistent with the generation of product **2** inside cells, through a formal (2+2+2) multi-component annulation. Albeit the intramolecularity of the process might favor the annulation, we envisioned that once ruthenacycle intermediates like **B** (Figure 1b) are formed, they could be trapped with external alkynes (Figure 1, v). Gratifyingly, treatment of diyne **3** with terminal alkyne **4a**

(4 equiv), in water, gave the expected phthalan-like product in 60% yield, after only 2 h, using 25% of **Ru1** (Figure 3a). The yield increases up to 94% when the reaction is carried out in a phosphate-buffered saline solution (PBS). The reaction also takes place in DMEM and in presence of HeLa cell lysates (95% and 89% yields, respectively, Figure 3a), and can be promoted with other complexes like [RuCp-(CH$_3$CN)$_3$]PF$_6$ or **Ru2**, which gave the product in modest yields of 38 and 14% (respectively) in PBS (Table S1).

The success of the reaction with the model precursor **3**, prompted us to investigate the generation of fluorescent and/or biologically relevant products. In particular, we were attracted by anthraquinone skeletons (AQ), as they form the core of many attractive secondary metabolites that have found relevant biomedical applications.[17]

The AQ skeleton could be assembled in a single step by means of a Ru-promoted annulation between bispropargylic ketones of type **6** and alkynes (Figure 3a, bottom).[18] In nature, the main polycyclic core of AQs is biosynthesized from acetylCoA and malonylCoA, in a multistep process governed by the multi-domain enzyme polyketide synthase (PKs) present in some plants, fungi, insects and bacteria (Figure 3b). However, mammalian cells do not code for the biosynthesis of AQs, which added further interest to explore the possibility of building these products inside these cells.

Gratifyingly, the bispropargylic ketone **6a** reacted with commercially available alkyne **4a** (4 equiv) in presence of **Ru1** (50%) to give the expected tricycle **7a** in 79% yield after 2 h at rt, in water (Figure 3a, bottom). The catalyst loading can be reduced to 25%, albeit there is a decrease in the yield (59%). Importantly, the concentration of **6a** could be decreased to 500 μM (53% yield). The reaction can be also accomplished in PBS even at 25% of **Ru1** (65% yield). In cell culture media, such as DMEM, or in HeLa cell lysates the reaction presents almost no turnover (37 and 28% respectively, using 25% of **Ru1**). The cycloaddition is also feasible using an internal 1,6-diyne such as **6b**, albeit it was somewhat slower (45% yield, using 50% of **Ru1** in water). In this case, we found that the use of an organic co-solvent (H$_2$O/MeCN 8:2), allowed a slightly better yield (59%). Other terminal alkynes (**4**) also participate in the cycloaddition (Table S3).
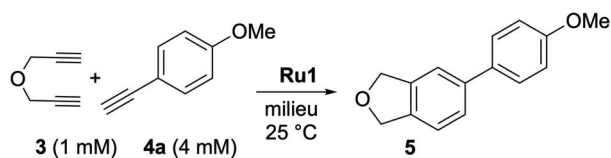
Substrates **6a** and **4a** are not fluorescent, however the anthraquinone product **7a** presents bright green and blue fluorescence emission, which facilitates monitorization in cellular settings. For cellular experiments we preferred to use **Ru2**, owing to its better uptake[5e] (although catalyst **Ru1** was also able to elicit the reaction in HeLa cells, Figure S10). These experiments were carried out by incubating the cells with **Ru2**, followed by treatment with alkyne **4a** and diyne **6a** (Figure 4a and S9). After 4 h, we were glad to observe an intense fluorescence build-up inside the cells, consistent with the formation of anthraquinone product **7a** (Figure 4a, panels A, B).

Control experiments confirmed that addition of anthraquinone product **7a** to HeLa cells elicits a clear intracellular fluorescence (panel D, Figure 4a). In contrast, cells co-incubated with substrates **6a** and **4a** were nearly non-fluorescent (Figure 4a, panel C). As expected, addition of each component alone, either **6a** or **4a**, to cells that had been previously treated with the ruthenium reagent, led only to residual intracellular fluorescence (arising from the substrates, Figure S10).
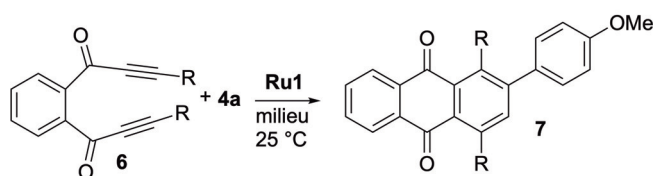
The intracellular formation of AQ products was further confirmed by carrying out the reaction with the alkyne derivative **4P**, which features a phosphonium tail (Figure 4b). This group facilitates the identification of the product owing to its good performance in ESI-MS spectrometry. Therefore, MS analysis (extracted ion chromatogram) of methanolic extracts of cells treated with **4P**, and either **3** or **6a**, under the standard reaction conditions, revealed the presence of the expected cycloadducts (Figure 4b, Section S14). These results suggest that this type of molecular labels (phosphonium cations or similar), could allow to overcome the current limitation of detection tactics to fluorescent products.

To further expand the scope and potential of the technology, we envisioned the synthesis of products with tetraphenylethylene skeletons like **9a**, using alkyne **8a** as reaction partner (Figure 5a).

a) Intermolecular cycloadditions^a

Diyne	R	% **Ru1**	milieu	% yield
6a	H	50	H$_2$O	79
6a	H	25	H$_2$O	59
6a	H	25	PBS	65
6a	H	25	DMEM	37
6a	H	25	Lysates	28
6b	Me	50	H$_2$O	45
6b	Me	50	PBS	48
6b	Me	50	H$_2$O/CH$_3$CN	59

For compound **5**:

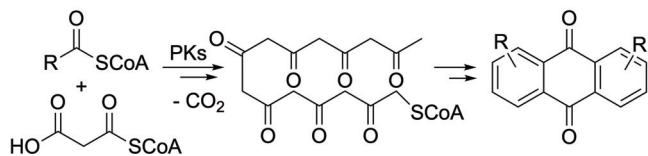|	H$_2$O	PBS	DMEM	Lysates^b
yield (%)	60	94	95	89

b) Anthraquinone biosynthesis

Figure 3. a) Formal (2+2+2) cycloadditions in complex aqueous media. b) Plausible biological pathway for the synthesis of anthraquinones. [a] Performed using substrate **3** or **6** (5 μmol), milieu (5.0 mL), 25°C, 2 h; [b] Cell lysates 2 mg mL^{-1}; Yields determined by NMR spectroscopy using an internal standard. Number of replicates: between 2 and 4, and errors in yields range between 3–6%.

a) Intracellular generation of product **7a**
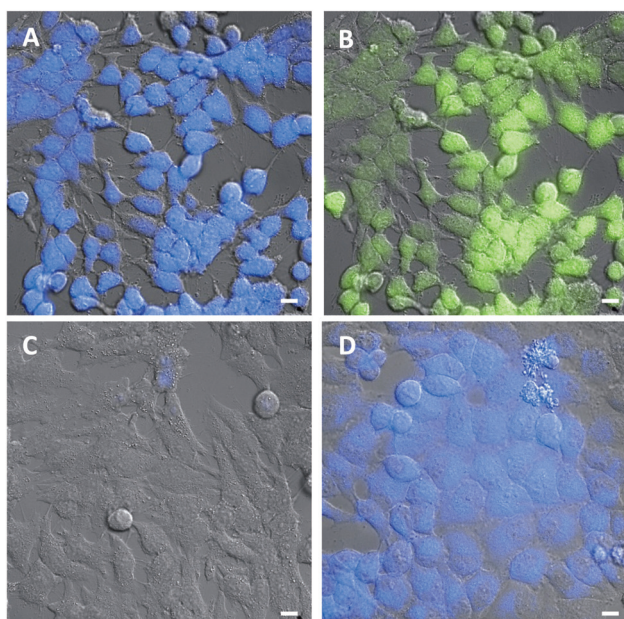
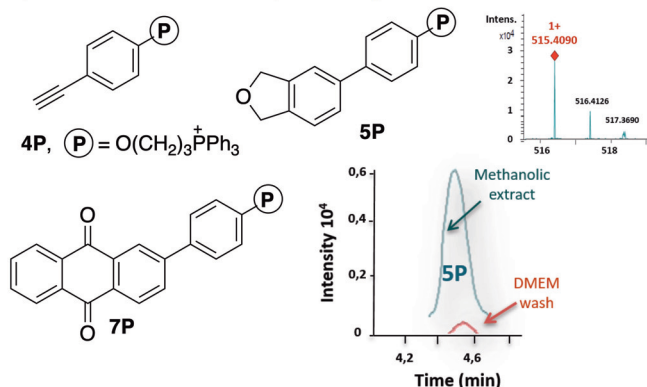b) Detection of intracellular products by LC/MS

Figure 4. Intermolecular cycloadditions in live cells. a) Fluorescence micrographies of HeLa cells (brightfield) after incubation with: A) **Ru2**, washed, and treated with **6a** and **4a**; B) similar, but observation under the green channel; C) **6a** and **4a**; D) product **7a**. b) Products with the triphenylphosphonium tails. Extracted ion chromatogram of the product **5P** generated intracellularly (methanolic extract) and also that detected in the DMEM washings, before the extraction; (inset) mass spectrum of **5P**. Conditions: HeLa cells pretreated with 50 μM of **Ru2** for 50 min were washed twice and incubated with 50 μM of substrate (**3a** or **6a**) and 150 μM of alkynes (either **4a** or **4P**) for 4 h. Blue channel: $\lambda_{exc} = 385$ nm, $\lambda_{em} = 410$–480 nm; green channel: $\lambda_{exc} = 470$ nm, $\lambda_{em} = 490$–580 nm. Scale bar: 12.5 μm.

This type of structures, known to present aggregation-induced emission properties (AIE),[19] are very attractive from a photophysical perspective.[20] Unfortunately, while the alkyne **8a** displays an excellent emission, the corresponding cycloadduct **9a** presents a strong decrease in its AIEgen properties, perhaps because of an increased molecular rotation (Figure S11). However, AQ **9b**, obtained from alkyne **8b**, behaves as an excellent AIEgen (Figure 5a, Figure S12).

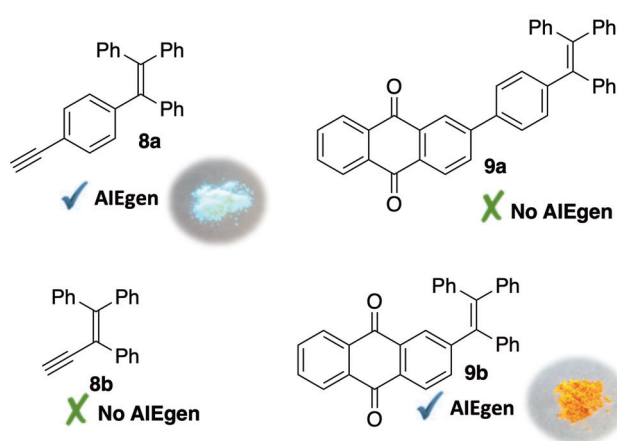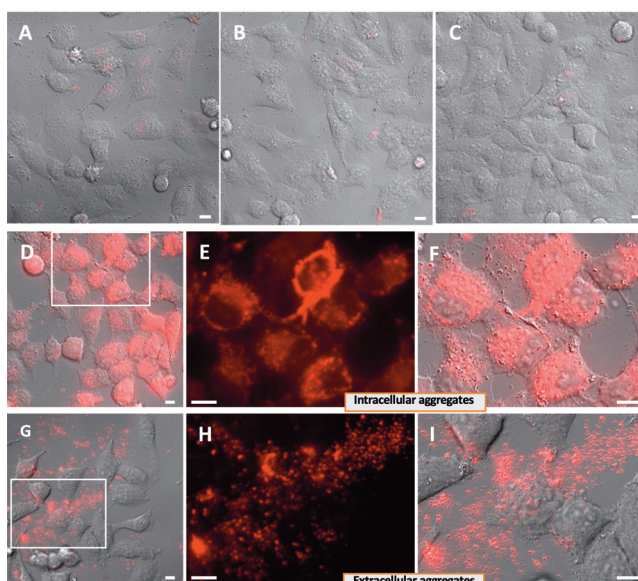a) Assembly of AIEgens using (2+2+2) cycloadditions

b) Intracellular generation of AIEgen **9b**

Figure 5. Intracellular generation of AIEgens. a) Structures of the precursors and cycloaddition products. b) Fluorescence micrographies of HeLa cells (brightfield) after incubation with: A) **Ru2**, washed, and treated with **6a**; B) **Ru2**, washed, and treated with **8b**; C) precursors **6a** and **8b**; D) **Ru2**, washed, and treated with **6a** and **8b**; E,F) Zoom in of panel D; G) anthraquinone **9b**; H,I) Zoom in of panel G. Conditions: HeLa cells were incubated with **Ru2** (50 μM) for 1 h, followed by two washings with DMEM, and treatment with substrates **6a** and **8** (50 and 150 μM, respectively) for 3 h. Red channel: $\lambda_{exc} = 550$ nm, $\lambda_{em} = 570$–690 nm. Scale bar: 12.5 μm.

Importantly, the product (**9b**) can be generated inside live mammalian cells using the cyclotrimerization reaction. Therefore, the addition of substrates **6a** and **8b** to HeLa cells previously treated with the ruthenium complex **Ru2**, leads to an intense intracellular red staining (Figure 5b, panel D, enlarged images in E, F). This result is especially significant because the anthraquinone **9b** is unable to travel inside cells. Indeed, incubation of cells with the anthraquinone **9b** leads to the formation of aggregates in the extracellular media (Figure 5b, panel G, and enlarged images in H, I). This product can be internalized only after permeabilization of the

membrane with digitonin (Figure S16). Therefore, our approach allows to indirectly introduce in cells a product (anthraquinone **9b**) that otherwise aggregates in the extracellular space. Importantly, these results further corroborate the intracellular character of the reaction.

An additional asset of the strategy stems from the possibility of controlling the intracellular distribution of the AQ product **9b** depending on the ruthenium reagent. Therefore, by using complex **Ru1**, the cellular fluorescence shows a cytosolic profile (slightly less intense than with **Ru2**, Figure 6, panels A–C). However, using complex **Ru3**, which is known to preferentially accumulate in mitochondria owing to its lipophilic cationic character,[5e] the fluorescence is mainly located in these organelles (Figure 6, panels D–F, Figure S13).
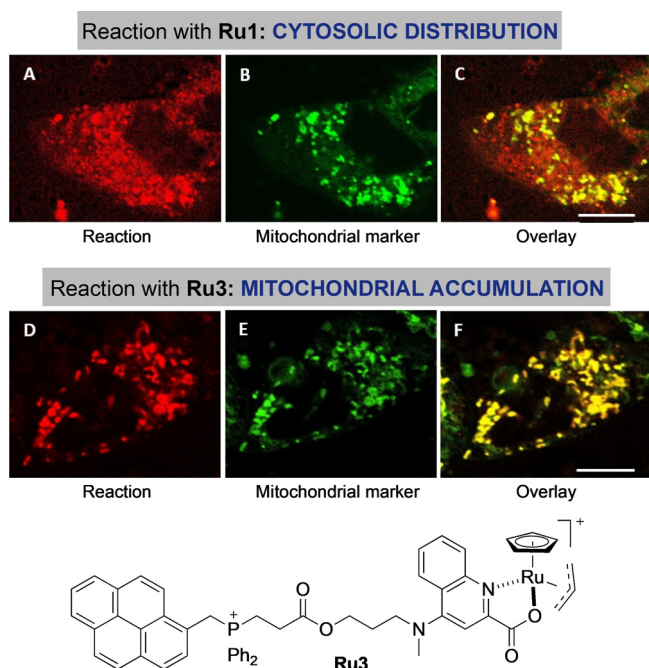

Reaction with Ru1: CYTOSOLIC DISTRIBUTION

A — Reaction   B — Mitochondrial marker   C — Overlay

Reaction with Ru3: MITOCHONDRIAL ACCUMULATION

D — Reaction   E — Mitochondrial marker   F — Overlay

Figure 6. Reagent-dependent spatial distribution of the product of the reaction between **6a** and **8b**. Fluorescence micrographies of HeLa cells incubated with: A,D) **Ru1** or **Ru3**, respectively, washed, and treated with **6a** and **8b** (red channel); B,E) mitochondrial labelling with TMRE (tetramethylrhodamine ethyl ester, green channel); C) overlay of A and B; F) overlay of D and E. Same conditions as in Figure 5. Cells were finally incubated with mitochondrial marker (100 nM) for 10 min. Scale bar: 12.5 μm. Note: counterions in **Ru3** are Br$^-$ and PF$_6$$^-$.

Finally, it is important to note that in all the above experiments neither substrates nor products compromised the cell viability at the observation times, inducing only a slight decrease after 12 h of incubation at high concentrations (Figure S8).[5e]

Conclusion

In conclusion, our results demonstrate that transition metals can promote challenging (2+2+2) multicomponent cycloadditions in live mammalian cells. The use of abiotic reactants with bidentate metal coordination abilities (diyne) seems instrumental for the success of the process. In addition to provide a cutting-edge addition to the palette of cell-compatible metal-mediated transformations, our work demonstrates the viability of synthesizing complex, biorelevant polycycles inside cells from simple precursors, and therefore goes beyond the more common uncaging or ligation reactions. Our intracellular synthetic strategy allows to generate products that otherwise cannot be delivered to the cell, as well as controlling their spatial distribution by using suitable ruthenium reagents. Indeed, the possibility of generating the desired products in specific subcellular locations, just by changing the targeting characteristics of the reagents, is exciting. While further work to increase the efficiency of the reactions is needed, our discoveries should further foster this young field of intracellular metal catalysis, and trigger important applications in chemical and synthetic biology, and in biomedicine.

Conflict of interest

The authors declare no conflict of interest.

[1] a) S. Martínez Cuesta, S. A. Rahman, N. Furnham, J. M. Thornton, *Biophys. J.* **2015**, *109*, 1082–1086; b) B. Alberts, A. Johnson, J. Lewis, D. Morgan, M. Raff, K. Roberts, P. Walter in *Molecular biology of the cell*, 6th ed., Garland Science, New York, **2017**.
[2] a) M. T. Reetz, *Acc. Chem. Res.* **2019**, *52*, 336–344; b) F. Schwizer, Y. Okamoto, T. Heinisch, Y. Gu, M. M. Pellizzoni, V. Lebrun, R. Reuter, V. Köhler, J. C. Lewis, T. R. Ward, *Chem. Rev.* **2018**, *118*, 142–231; c) M. Jeschek, S. Panke, T. R. Ward, *Trends Biotechnol.* **2018**, *36*, 60–72; d) R. B. Leveson-Gower, C. Mayer, G. Roelfes, *Nat. Rev. Chem.* **2019**, *3*, 687–705.

[3] a) M. Yang, J. Li, P. R. Chen, *Chem. Soc. Rev.* **2014**, *43*, 6511–6526; b) J. Li, J. Yu, J. Zhao, J. Wang, S. Zheng, S. Lin, L. Chen, M. Yang, S. Jia, X. Zhang, P. R. Cheng, *Nat. Chem.* **2014**, *6*, 352–361; c) J. Wang, B. Cheng, J. Li, Z. Zhang, W. Hong, X. Chen, P. R. Chen, *Angew. Chem. Int. Ed.* **2015**, *54*, 5364–5368; *Angew. Chem.* **2015**, *127*, 5454–5458; d) A. M. Pérez-López, B. Rubio-Ruiz, V. Sebastián, L. Hamilton, C. Adam, T. L. Bray, S. Irusta, P. M. Brennan, G. C. Lloyd-Jones, D. Sieger, J. Santamaría, A. Unciti-Broceta, *Angew. Chem. Int. Ed.* **2017**, *56*, 12548–12552; *Angew. Chem.* **2017**, *129*, 12722–12726; e) C. Adam, A. M. Pérez-López, L. Hamilton, B. Rubio-Ruiz, T. L. Bray, D. Sieger, P. M. Brennan, A. Unciti-Broceta, *Chem. Eur. J.* **2018**, *24*, 16783–16790; f) M. Sancho-Abero, B. Rubio-Ruiz, A. M. Pérez-López, V. Sebastián, P. Martín-Duque, M. Arruebo, J. Santamaría, A. Unciti-Broceta, *Nat. Catal.* **2019**, *2*, 864–872.

[4] For recent reviews, see: a) M. Martínez-Calvo, J. L. Mascareñas, *Coord. Chem. Rev.* **2018**, *359*, 57–79; b) A. H. Ngo, S. Bose, L. H. Do, *Chem. Eur. J.* **2018**, *24*, 10584–10594; c) Y. Bai, J. Chen, S. C. Zimmerman, *Chem. Soc. Rev.* **2018**, *47*, 1811–1821; d) J. J. Soldevilla-Barreda, N. Metzler-Nolte, *Chem. Rev.* **2019**, *119*, 829–869; e) M. Martínez-Calvo, J. L. Mascareñas, *Chimia* **2018**, *72*, 791–801.

[5] a) C. Streu, E. Meggers, *Angew. Chem. Int. Ed.* **2006**, *45*, 5645–5648; *Angew. Chem.* **2006**, *118*, 5773–5776; b) T. Völker, F. Dempwolff, P. L. Graumann, E. Meggers, *Angew. Chem. Int. Ed.* **2014**, *53*, 10536–10540; *Angew. Chem.* **2014**, *126*, 10705–10710; c) M. I. Sánchez, C. Penas, M. E. Vázquez, J. L. Mascareñas, *Chem. Sci.* **2014**, *5*, 1901–1907; d) G. Y. Tonga, Y. Jeong, B. Duncan, T. Mizuhara, R. Mout, R. Das, S. T. Kim, Y. C. Yeh, B. Yan, S. Hou, V. M. Rotello, *Nat. Chem.* **2015**, *7*, 597–603; e) M. Tomás-Gamasa, M. Martínez-Calvo, J. R. Couceiro, J. L. Mascareñas, *Nat. Commun.* **2016**, *7*, 12538–12547; f) M. Martínez-Calvo, J. R. Couceiro, P. Destito, J. Rodríguez, J. Mosquera, J. L. Mascareñas, *ACS Catal.* **2018**, *8*, 6055–6061; g) B. J. Stenton, B. L. Oliveira, M. J. Matos, L. Sinatra, G. J. L. Bernardes, *Chem. Sci.* **2018**, *9*, 4185–4189; h) S. Learte-Aymamí, C. Vidal, A. Gutiérrez-González, J. L. Mascareñas, *Angew. Chem. Int. Ed.* **2020**, *59*, 9149–9154; i) P. Destito, A. Sousa-Castillo, J. R. Couceiro, F. López, M. A. Correa-Duarte, J. L. Mascareñas, *Chem. Sci.* **2019**, *10*, 2598–2603; j) R. Martínez, C. Carrillo-Carrión, P. Destito, A. Álvarez, M. Tomás-Gamasa, B. Peláz, F. López, J. L. Mascareñas, P. Del Pino, *Cell Rep. Phys. Sci.* **2020**, *1*, 100076.

[6] a) J. J. Soldevila-Barreda, I. Romero-Canelon, A. Habtemariam, P. J. Sadler, *Nat. Commun.* **2015**, *6*, 6582–6590; b) J. P. C. Coverdale, I. Romero-Canelon, C. Sanchez-Cano, G. J. Clarkson, A. Habtemariam, M. Wills, P. J. Sadler, *Nat. Chem.* **2018**, *10*, 347–354; c) S. Bose, A. H. Ngo, L. Do, *J. Am. Chem. Soc.* **2017**, *139*, 8792–8795.

[7] C. Vidal, M. Tomás-Gamasa, A. Gutiérrez-González, J. L. Mascareñas, *J. Am. Chem. Soc.* **2019**, *141*, 5125–5129.

[8] a) C. Vidal, M. Tomás-Gamasa, P. Destito, F. López, J. L. Mascareñas, *Nat. Commun.* **2018**, *9*, 1913–1921; b) M. A. Miller, B. Askevold, H. Mikula, R. H. Kohler, D. Pirovich, R. Weissleder, *Nat. Commun.* **2017**, *8*, 15906–15918.

[9] There have been claims on the existence of Diels–Alderases: a) A. Minami, H. Oikawa, *J. Antibiot.* **2016**, *69*, 500–506, b) H. Oikawa, *Cell Chem. Biol.* **2016**, *23*, 429–430.

[10] a) A. J. Link, D. A. Tirrell, *J. Am. Chem. Soc.* **2003**, *125*, 11164–11165; b) A. J. Link, M. K. S. Vink, D. A. Tirrell, *J. Am. Chem. Soc.* **2004**, *126*, 10598–10602; c) K. E. Beatty, F. Xie, Q. Wang, D. A. Tirrell, *J. Am. Chem. Soc.* **2005**, *127*, 14150–14151; d) Y. Bai, X. Feng, H. Xing, Y. Xu, B. K. Kim, N. Baig, T. Zhou, A. A. Gewirth, Y. Lu, E. Oldfield, S. C. Zimmerman, *J. Am. Chem. Soc.* **2016**, *138*, 11077–10080; e) S. Li, L. Wang, F. Yu, Z. Zhu, D.

Shobaki, H. Chen, M. Wang, J. Wang, G. Qin, U. J. Erasquin, L. Ren, Y. Wang, C. Cai, *Chem. Sci.* **2017**, *8*, 2107–2114; f) J. Miguel-Ávila, M. Tomás-Gamasa, A. Olmos, P. J. Pérez, J. L. Mascareñas, *Chem. Sci.* **2018**, *9*, 1947–1952.

[11] a) E. M. Sletten, C. R. Bertozzi, *Angew. Chem. Int. Ed.* **2009**, *48*, 6974–6998; *Angew. Chem.* **2009**, *121*, 7108–7133; b) D. M. Patterson, J. A. Prescher, *Curr. Opin. Chem. Biol.* **2015**, *28*, 141–149; c) N. K. Devaraj, *ACS Cent. Sci.* **2018**, *4*, 952–959.

[12] P. Destito, J. R. Couceiro, H. Faustino, F. López, J. L. Mascareñas, *Angew. Chem. Int. Ed.* **2017**, *56*, 10766–10770; *Angew. Chem.* **2017**, *129*, 10906–10910.

[13] Chelating ligands have been useful in Cu click chemistry: a) C. Uttamapinant, A. Tangpeerachaikul, S. Grecian, S. Clarke, U. Singh, P. Slade, K. R. Gee, A. Y. Ting, *Angew. Chem. Int. Ed.* **2012**, *51*, 5852–5856; *Angew. Chem.* **2012**, *124*, 5954–5958; b) V. Bevilacqua, M. King, M. Chaumontet, M. Nothisen, S. Gabillet, D. Buisson, C. Puente, A. Wagner, F. Taran, *Angew. Chem. Int. Ed.* **2014**, *53*, 5872–5876; *Angew. Chem.* **2014**, *126*, 5982–5986; c) T. Machida, N. Winssinger, *ChemBioChem* **2016**, *17*, 811–815; d) Y. Su, L. Li, H. Wang, X. Wang, Z. Zhang, *Chem. Commun.* **2016**, *52*, 2185–2188.

[14] For reviews on metal-catalyzed (2+2+2) cycloadditions, see: a) M. Lautens, W. Klute, W. Tam, *Chem. Rev.* **1996**, *96*, 49–92; b) Y. Yamamoto, *Curr. Org. Chem.* **2005**, *9*, 503–519; c) S. Kotha, E. Brahmachary, K. Lahiri, *Eur. J. Org. Chem.* **2005**, 4741–4767; d) P. R. Chopade, J. Louie, *Adv. Synth. Catal.* **2006**, *348*, 2307–2327; e) B. R. Galan, T. Rovis, *Angew. Chem. Int. Ed.* **2009**, *48*, 2830–2834; *Angew. Chem.* **2009**, *121*, 2870–2874; f) G. Domínguez, J. Pérez-Castells, *Chem. Soc. Rev.* **2011**, *40*, 3430–3444; g) Y. Shibata, K. Tanaka, *Synthesis* **2012**, *44*, 323–350.

[15] a) H. Kinoshita, H. Shinokubo, K. Oshima, *J. Am. Chem. Soc.* **2003**, *125*, 7784–7785; b) V. Cadierno, S. E. García-Garrido, J. Gimeno, *J. Am. Chem. Soc.* **2006**, *128*, 15094–15095; c) F. Xu, C. Wang, X. Li, B. Wan, *ChemSusChem* **2012**, *5*, 854–857; d) Z. Nairoukh, M. Fanun, M. Schwarze, R. Schomäcker, J. Blum, *J. Mol. Catal. A* **2014**, *382*, 93–98; e) J. Francos, S. E. García-Garrido, J. García-Álvarez, P. Crochet, J. Gimeno, V. Cadierno, *Inorg. Chim. Acta* **2017**, *455*, 398–414; f) C. R. Travis, G. H. Gaunt, E. A. King, D. D. Young, *ChemBioChem* **2020**, *21*, 310–314.

[16] a) L. Severa, J. Vávra, A. Kohoutova, M. Čížková, T. Šálová, J. Hývl, D. Šaman, R. Pohl, L. Adriaenssens, F. Teplý, *Tetrahedron Lett.* **2009**, *50*, 4526–4528; b) L. Adriaenssens, L. Severa, J. Vávra, T. Šálová, J. Hývl, M. Čížková, R. Pohl, D. Šaman, F. Teplý, *Collect. Czech. Chem. Commun.* **2009**, *74*, 1023–1034.

[17] G. Díaz-Muñoz, I. L. Miranda, S. K. Sartori, D. C. de Rezende, M. A. N. Díaz, *Stud. Nat. Prod. Chem.* **2018**, *58*, 313–338.

[18] Y. Yamamoto, K. Hata, T. Arakawa, K. Ito, *Chem. Commun.* **2003**, 1290–1291.

[19] a) W. Chen, C. Zhang, X. Han, S. H. Liu, Y. Tan, J. Yin, *J. Org. Chem.* **2019**, *84*, 14498–14507; b) X. Gao, J. Z. Sun, Z. B. Tang, *Isr. J. Chem.* **2018**, *58*, 845–859; c) W. Xu, M. M. S. Lee, Z. Zhang, H. H. Y. Sung, I. D. Williams, R. T. K. Kwok, J. W. Y. Lam, D. Wang, B. Z. Tang, *Chem. Sci.* **2019**, *10*, 3494–3501.

[20] For recent reviews, see: a) J. Mei, N. L. C. Leung, R. T. K. Kwok, J. W. Y. Lam, B. Z. Tang, *Chem. Rev.* **2015**, *115*, 11718–11940; b) J. Mei, Y. Huang, H. Tian, *ACS Appl. Mater. Interfaces* **2018**, *10*, 12217–12261; c) Z. He, C. Ke, B. Z. Tang, *ACS Omega* **2018**, *3*, 3267–3277; d) Y. Chen, J. W. Y. Lam, R. T. K. Kwok, B. Liu, B. Z. Tang, *Mater. Horiz.* **2019**, *6*, 428–433.